Study of Vanadium (V) Adsorption Parameters from Aqueous Solution by Using Bare Magnetite Nanoparticles

Jalinousi, Yasaman
Faculty of Physics and Chemistry, Alzahra University, Tehran, I.R. IRAN

Saberyan, Kamal*+
Nuclear Fuel Cycle Research School, Nuclear Science and Technology Research Institute, Tehran, I.R. IRAN

Anafcheh, Maryam
Faculty of Physics and Chemistry, Alzahra University, Tehran, I.R. IRAN

ABSTRACT: *Heavy metals pollution in aquatic environments has increased significantly in the last few decades. Therefore, different technologies have been used to deal with this problem. In these technologies, different adsorbents are used to adsorb and separate heavy metals from the aqueous medium. In this regard, the use of new technologies such as nanomaterial technology which uses nanomaterials as adsorbents with potential for adsorption capacity and fast recovery and low cost, especially magnetite nanoparticle adsorbents, has provided efficient and cost-effective solutions for the extraction and removal of heavy metals from water. In the present study, the separation of vanadium (V) in aqueous medium was studied using an adsorbent of magnetite nanoparticles that was successfully synthesized by co-precipitation method. The synthesized nanoparticles were tested without functionalization to remove vanadium. The maximum adsorption percentage of vanadium by non-functionalized magnetite nanoparticles was 99.6 percent in optimum conditions: pH equal to 3.5, at ambient temperature (20 °C), contact time 30 minutes, 5000 mg/L adsorbent amount, and 50 mg/L initial concentration of vanadium (V). The Langmuir, Freundlich and Temkin isotherm models were evaluated for vanadium adsorption process. It was observed that the Langmuir isotherm fitted better onto the laboratory data than other models. The kinetics of the experiment showed that the data obtained were more consistent with the pseudo-second-order kinetic model.*

KEYWORDS: *Adsorption; Desorption; Vanadium; Magnetite nanoparticles.*

INTRODUCTION

Vanadium has an unusually large number of stable oxidation states (+2, +3, +4, +5), each of which is characterized by a unique color in solution. But it is mainly found in the form of quaternary and pentavalent species in the environment.

**To whom correspondence should be addressed.*
+ E-mail: saberyan@aeoi.org.ir
1021-9986/2023/9/2896-2911 16/$/6.06

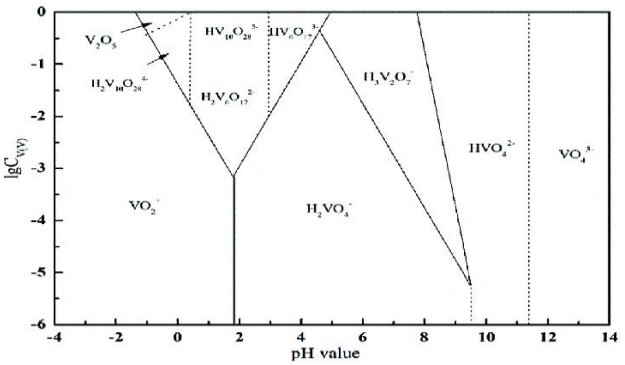

Fig. 1: Effect of concentration and pH value on pentavalent vanadium morphology [11]

This metal is used as an alloying agent for steel. It combines with nearly all non-metals in compounds. Vanadium is a refractory metal and the melting point of this metal can reach 1890 °C [1]. According to important national strategy sources, vanadium and their compounds were widely used in iron steel, catalysts, and the petrochemical industry due to their excellent physicochemical properties; therefore, vanadium was called the "vitamin of modern industry" [2-5]. To date, the main raw materials for vanadium recovery we are converter vanadium slag, stone coat, steel slag and waste catalyst materials [6,7].

Vanadium metal enters in the manufacturing of some superconducting alloys and its addition to iron makes many stainless steel materials. The disproportionation of CO into C and CO_2 needs vanadium to catalyze the reaction. Vanadium oxide is a strong catalyst, so it is largely used in industrial processes and finding recent applications in nanomaterials [8]. Vanadium is found in natural waters in many distinct forms, V(IV) and V(V) have been varying biological and toxic properties. At low pH ($< 2-3$), vanadium(V) occurs mostly as a cation (VO_2^+), whereas the anionic species exist at higher pH values (>3): the decavanadate species $V_{10}O_{28}(OH)_2^{4-}$, $V_{10}O_{27}(OH)^{5-}$and mono- or polyvanadate species (e.g. $VO_2(OH)_2^-$, $VO_3(OH)^{2-}$,VO_4^{3-}, and $V_2O_6(OH)^{3-}$, $V_2O_7^{4-}$, $V_3O_9^{3-}$, $V_4O_{12}^{4-}$) [9]**.** The concentration of vanadium entering the freshwater from effluents and leachates (0.2–100 µg/L) is far higher than its concentration in seawater (1–3 µg/L) which tends to precipitate, while groundwater samples from volcanic regions have high vanadium concentrations, ranging from 0.05 to 2.47 mg/L [10]**.** Fig. 1 represents that the dissolved vanadium concentration had a certain impact on the existing form of vanadium.

Therefore, considering the negative impacts of Heavy Metals (HMs) on human health and the environment, it is necessary to introduce a cost-effective, environmental-friendly and efficient processes for the removal of HMs from the contaminated water. The treatment processes for waste solutions containing metals like vanadium generally includes chemical precipitation, filtration, membrane, ion exchange and adsorption [12]. At present the adsorption and ion exchange techniques have become the focus in the field of harmless and safe treatment of heavy metals refers to their large capacity, high efficiency, low cost and environmental friendliness [13]. Adsorption is a mass transfer process, where the adsorbate molecules are attracted to the surface of an adsorbent, resulting in either a physical or chemical interaction. It is one of the most favored processes in the water treatment industry, especially due to the regenerative capacity of the adsorbents [14, 15].

In fact, the adsorption capacity varies with the type of adsorbent. Generally, there are many existential adsorbents, activated carbon due to its high adsorption rate, capacity and resistance to abrasion are extensively used for the removal of heavy metals. But due to their clogging, inability to recover them from the treated water, waste generation, and biofouling, they are ineffective for large scale applications [16]. Therefore, the search for new and effective adsorbent materials has always been an active field of research. Nanomaterials, due to their nanoscale dimensions (ranging from 1–100 nm), show some unique physical, chemical and biological properties. These properties result in the modification of their structure and specific surfaces [17]. Nanomaterials are classified into different categories, i.e., carbon based, silica based, metal and metal oxide nanoparticles, including zero-valent iron (ZVI), iron-oxide based magnetic nanomaterials, and nanocomposites, as shown in Fig. 2.

For instance, *Popescu et al.* They reported the maximum uranium adsorption capacity using carboxymethyl cellulose with and without iron oxide nanoparticles as 322.6 mg/g and 185.2 mg/g, respectively [19].

Even though the nanomaterials have an enormous capacity in the extraction of heavy metals, they carry certain limitations with regards to their cost effectiveness,

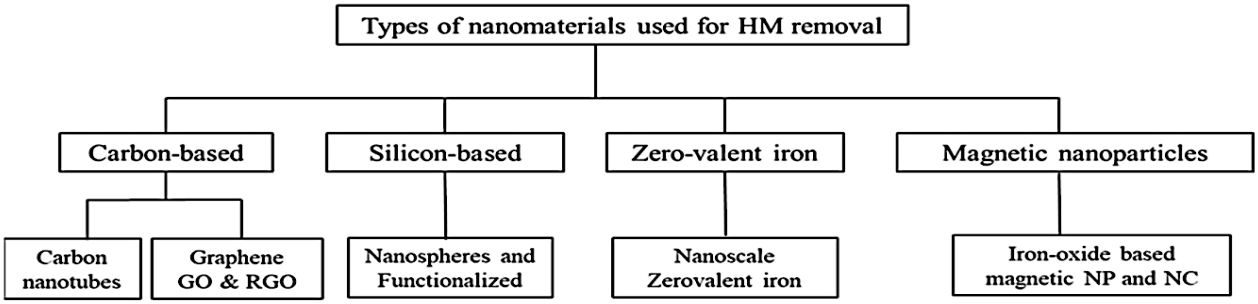

Fig. 2: Nanomaterials for heavy metals remediation in aqueous media [18]

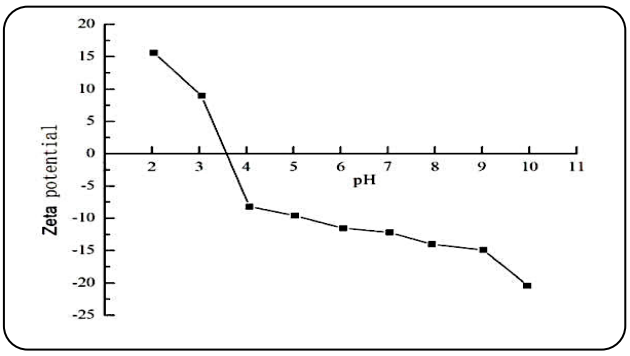

Fig. 3: Effect of pH on zeta potential of Fe_3O_4 [27]

reusability, separation from aqueous solutions, and complex synthesis routes, which impede their utilization at a commercial scale [20].

During the last two decades, micro and Nano-scaled magnetic particles have attracted attention as adsorbents for eliminating the biological molecules, organic pollutants and heavy metal ions like as vanadium from water and wastewater [21].

Among the magnetic materials, magnetic iron-oxide NP, i.e., magnetite (Fe_3O_4) and maghemite (γ-Fe_2O_3) present substantial dominance over conventionally used metal and alloy based on magnetized nanomaterials in terms of facile synthesis, corrosion and abrasion resistance. Maghemite and magnetite NP are extensively studied for wastewater treatment and heavy metal ion like vanadium removal [22]. For example, *Zeinali et al.* using magnetite nano-adsorbent coated with humic acid, they succeeded in removing more than 93% of vanadium from the power plant effluent [23]. In this study, we will also investigate the removal of vanadium by using magnetite nanoparticle adsorbents. Among the magnetic metals (iron, cobalt, nickel, etc.), iron is the cheapest metal. Therefore, it is recommended to use iron for processes such as adsorption and separation, which is one of the main goals is reducing the cost of the process, especially on an industrial scale. The most iron oxides that have been used for the adsorption process are magnetite and maghemite, among these two oxides, because magnetite has more magnetization than maghemite, it has received more attention which was consistent with some studies reported (*Zeinali et al.* [23]; *Gdula et al.* [24]). As explained in the second line, the first paragraph of the "Introduction" section, although vanadium has four oxidation numbers (+2, +3, +4 and +5), but mainly vanadium is in the form of +4 and +5 oxidation states (more stable oxidation numbers. (Among the two oxidation numbers of +4 and +5, usually due to the oxidizing nature of the environment (waste, environment and the leach solution), Vanadium often has the oxidation number of +5. Therefore, vanadium +5 was selected to work by the researchers of this article. *Zeinali et al.* [23]; *Omidinasab et al.* [25]; *Kordparijaei et al.* [26]) studied the adsorption of vanadium in the form of vanadium (V) as in the present research project. Since in this project the surface adsorption of vanadium on magnetite nanoparticles adsorbent has been investigated, it should be pointed out the pH had a significant impact on adsorption of metal ions on Fe_3O_4. pH value affected the surface zeta potential of Fe_3O_4 particles. When the pH increased from 2.0 to 5.0, the surface zeta potential of Fe_3O_4 particles decreased. The surface zeta potential of Fe_3O_4 changed from positive to negative, and the isoelectric point (pHpzc) occurred at pH of 3.0–4.0 (Fig. 3).

In an aqueous system, the surface of iron oxides is covered with groups of −FeOH, etc. [28]. Since the adsorbent

surface was not functionalized in this project, the vanadium ion was adsorbed to the −FeOH groups on the adsorbent surface. When the pH value was below or above the pHpzc, hydroxyl groups of −FeOH on the surface would be changed to functional groups of $FeOH_2^+$ or FeO^- by protonate or deprotonate [29]. The balance of protonation and deprotonation depended on the pH of the solution and the pHpzc of Fe_3O_4. When pH was 3.0–4.0, the zeta potential was almost the smallest, and the adsorption was easier to carry out.

EXPERIMENTAL SECTION

Reagents and apparatus

The following reagents were used: iron(II) sulfate heptahydrate ($FeSO_4 \cdot 7H_2O$), Ammonium iron(III) sulfate dodecahydrate $NH_4\ Fe(SO_4)_2 \cdot 12H_2O$, Polyethylene Glycol (PEG) 4000, Ammonia (25%) and hydrochloric acid (32%) were purchased from Merck Co. (KGaA, Darmstadt, Germany). The synthesized magnetite nanoparticles were characterized using techniques X-Ray Diffraction (XRD device, model Kristallo Flex Diffractometer D5000, Siemens company), Scanning Electron Microscope (SEM device equipped with EDS model Zeiss Ultra 55, Gemini) and Vibrating-Sample Magnetometer (VSM device model AGFM/VSM 3886).

Preparation of magnetite nanoparticles

The magnetite nanoparticles were synthesized through co-precipitation of ferric and ferrous ions in the presence of ammonia solution. Certain amounts of salts of $(NH_4)\ Fe(SO_4)_2 \cdot 12H_2O$ and $FeSO_4.7H_2O$ (Fe(III)/Fe(II)=2) were added to 20 mL of 0.6 M hydrochloric acid, along with 3 gr of PEG 4000.

The prepared solution was heated on a magnetic stirrer at 50-60 °C and simultaneously was stirred at 700 rpm. After the synthesis of magnetite nanoparticles according to Eq. (1), the black precipitate of magnetite, which was caused by titration with 25% ammonia, was washed three times with distilled water and then sonicated twice with an ultrasonic bath for 6 minutes. Then the nanoparticles were dried in an oven at 48°C for 24 hours.

$$Fe^{2+}(aq) + Fe^{3+}(aq) + 8NH_4OH(aq) \rightarrow Fe_3O_4 + 4H_2O + 8NH_4Cl \quad (1)$$

Adsorption experiments

Adsorption of V(V) ions was performed by the batch mode technique. In each experiment 10 mL of nanoparticle suspension (5000 mg/L of magnetite nanoparticles) was shaken with 10 mL of vanadium solution (50 mg/L of vanadium ion solution) for 30 min. Moreover, temperature influence on the adsorption process was also investigated at 293.15, 303.15, 313.15 and 323.15 K, and the pH-dependence was also examined. After the adsorption equilibrium had been achieved, the solution was separated from the adsorbent by a permanent magnet. Eq. (2) is used to calculate the adsorbed amount of vanadium ions:

$$q = (C_0 - C_e).{}^{V}/_{m} \quad (2)$$

where: q is the amount of adsorbed V(V) ions (mg/g), C_0 is the initial concentration of V(V) ions (mg/L), C_e is the equilibrium concentration of V(V) ions (mg/L), V is the volume of the initial solution (L), m is the mass of the adsorbent (g).

Characterization of the adsorbents

The XRD patterns of the adsorbent is shown in Fig. 4. Eight characteristic peaks of Fe_3O_4 with a spinel structure are identified by their indices: (533), (220), (311), (400), (422), (511), (440), and (622). These peaks are consistent with the database in JCPDS file (PDF No. 0863-003-00). This confirms the magnetic properties of the adsorbent [30]. The average size of the crystals was found to be 22 nm according to Scherer's Eq. (3) calculations.

$$d = \frac{K.\lambda}{\beta.cos\theta} \quad (3)$$

d is the mean size of the ordered (crystalline) domains (in nanometers), K is the shape factor has a typical value of about 0.9, λ is the X-ray wavelength (in terms of nanometers, if copper $K\alpha$ radiation is used, equal to 0.154 nm), β is the line broadening at half the maximum intensity (FWHM) after subtracting the instrumental line broadening in radians and θ is the Bragg angle (by degree) [31]. All peaks were placed according to JCPDS standards, which was the result of correct synthesis of magnetite nanoparticles.

It is known that magnetite nanoparticles possess magnetic properties. Thus the VSM method was applied in order to characterize them [32]. The obtained magnetization curves for the MNPs are given in Fig. 5. The maximum magnetization value for the MNPs is approx.

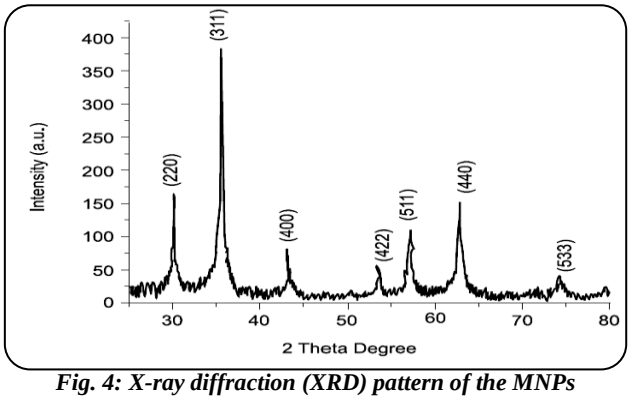

Fig. 4: X-ray diffraction (XRD) pattern of the MNPs

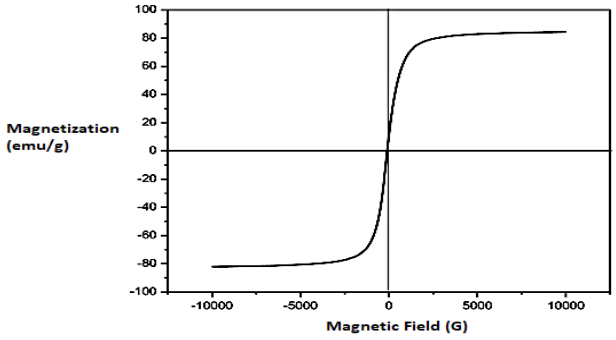

Fig. 5: Magnetization curves of MNPs obtained at 298 K

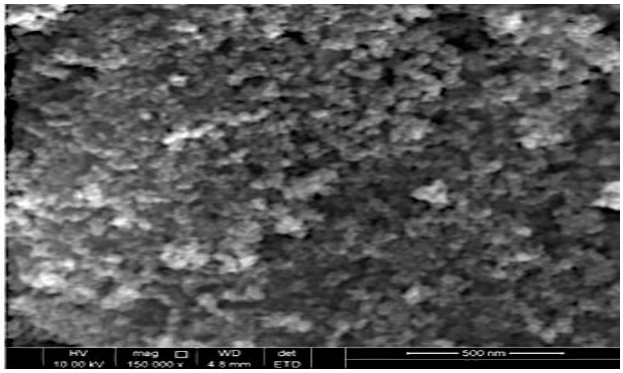

Fig. 6: SEM images of the synthesized nanoparticle

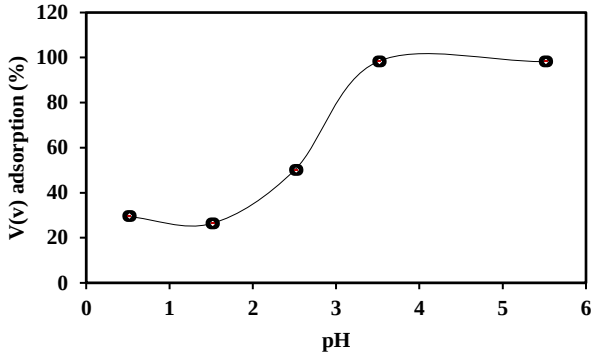

Fig. 7: Effect of pH on the adsorption of V(V) ions onto magnetite nanoparticles ($C_0(V)$ = 6 mg/L; T = room temperature; t = 30 min.; sorbent dosage= 0.05 g/L)

80 emu/g. Absence of remanence loop and zero remanence magnetism in magnetite nanoparticle magnetization curve obtained by VSM in Fig. 5 is proof of superparamagnetic of magnetite nanoparticle. High magnetic saturation indicates high magnetization, the value of which was obtained for the magnetite sample at an ambient temperature of 80 (emu/g).

The morphology and average size of the synthesized nanoparticles were obtained using SEM. Fig. 6 shows the SEM micrograph of the synthesized Fe_3O_4 nanoparticles. On the basis of the obtained microphotograph it can be concluded that co-precipitation of iron Fe^{2+} and Fe^{3+} ions results in formation of almost spherical Fe_3O_4 particles in the nanometer scale. It can be also seen that the average diameter distribution of nanoparticles in the magnetite sample was estimated to be 19 nm. The results we obtained from this SEM graph were consistent with the results of *Gdula et. al* [24].

RESULTS AND DISCUSSIONS

Effect of pH

In adsorption studies, the solution pH is known as a crucial controlling factor since it has significant effect on adsorbate ionization degree, solubility and speciation of the metal ions, change of functional groups of adsorbent, and surface charge of the adsorbent. Therefore, the effect of the initial pH of the aqueous solution on the removal efficiency of the metal ions was investigated in the pH range of 0.5 to 5.5, as illustrated in Fig. 7. This experiment was performed for vanadium solutions with pH 0.5, 1.5, 2.5, 3.5 and 5.5. The vanadium separation results are shown in Fig. 7. According to Fig. 8 the cationic chemical species VO_2^+ exist in the pH range between zero and approximately 3.5 and the results of Fig. 7 demonstrates that the lowest amount of vanadium adsorption is in the range of pH 0.5 to 2. The low amount of vanadium adsorption in this range is due to the high concentration of H^+ ion, which is more successful in competition with VO_2^+ ion for adsorption by nanoparticles. After adsorption, because the surface charge of the adsorbent becomes positive, the electrostatic repulsion between the VO_2^+ cation and the adsorbent surface prevents the adsorption of the VO_2^+ cation. However, in the range of pH 2 to 3.5 due to the decrease in H^+ ion concentration, VO_2^+ overcomes

Table 1: Effect of initial vanadium concentration on the aqueous phase (t= 30 min; T = room temperature; pH = 3.5; sorbent dosage= 0.5 g/L)

The value of the initial concentration of vanadium (mg/L)	% adsorption
5.6	99.6
9.3	99.6
18.7	99.6
50.0	99.6
93.3	91.0
186.6	58.0
466.5	39.3
933.0	21.0

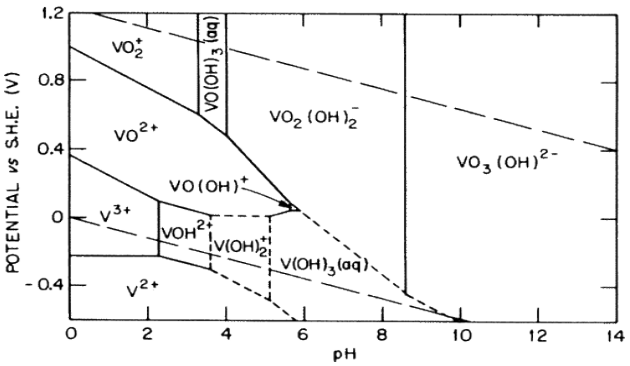

Fig. 8: Equilibrium dominant diagram of V(V)-OH species as a function of vanadium concentration and pH [36]

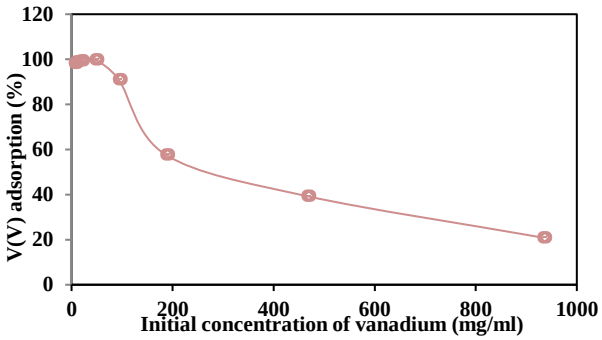

Fig. 9: Effect of initial vanadium concentration on the aqueous phase (t= 30 min; T = room temperature; pH = 3.5; sorbent dosage= 0.05 g/L)

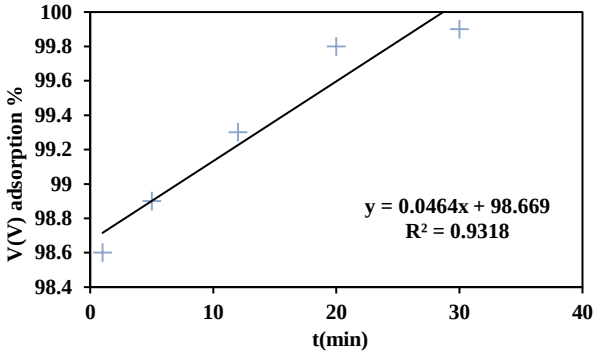

Fig. 10: Effect of contact time on adsorption process ($C_0(V)$ = 50 mg/L; sorbent dosage= 0.05 g/L; T = room temperature; pH = 3.5)

H^+ and the adsorption efficiency of this cation grows from approximately 30.0 to 99.6 percent. As the pH increases from 3.5 onwards, the adsorption value remains constant as shown in Fig. 7. Similar trends have been previously reported by other researchers for V(V) and other metal ions adsorption (*Mthombeni et al.* [33]; *Ahmadi et al.* [34]; *Omidinasab et al.* [25]; *Liu et al.* [35])

Effect of initial vanadium concentration on the adsorption efficient

The presence of vanadium ions has a significant effect on the vanadium recovery process. Therefore, it can be said that the removal of this metal from aqueous solutions depends to a large extent on its concentration [37]. The percentage of vanadium separation with adsorbent of magnetite nanoparticles in different initial concentrations of vanadium (5.6, 9.3, 18.7, 50.0, 93.3, 186.6, 466.5 and 933.0 mg/L) was investigated under the pre-assumption conditions. The results can be seen in Fig. 9. The adsorption percentage decreased with increasing initial vanadium concentration with saturation of specific adsorption sites at high metal concentrations, the decrease in adsorption at higher concentrations was clearly detectable, but at low concentrations, ions were adsorbed by specific adsorption sites. The concentration of 50 mg/L was considered as the optimal value of this experiment. In other words, it can be concluded that at higher concentrations of vanadium, due to the completion of the maximum adsorption capacity in the adsorbent, the adsorption percentage of this metal decreases, and the use of higher adsorbent values can solve this problem. Similar to the studies of (*Zeinali et al.* [23]; *Kordparijaei et al.* [26]), the adsorption efficiency decreased with the increase of the initial concentration of vanadium.

Effect of contact time and adsorption kinetics

Another important parameter is the adsorption kinetics because it is one of the most important criteria deciding about adsorbent efficiency. This also provides information about adsorption mechanism. Sorption of V(V) on magnetite nanoparticles was investigated as a function of

Table 2: The results of the vanadium separation percentage in different contact time

Contact Time (min)	Percentage of vanadium separation
1	98.6
5	98.9
12	99.3
20	99.8
30	99.9

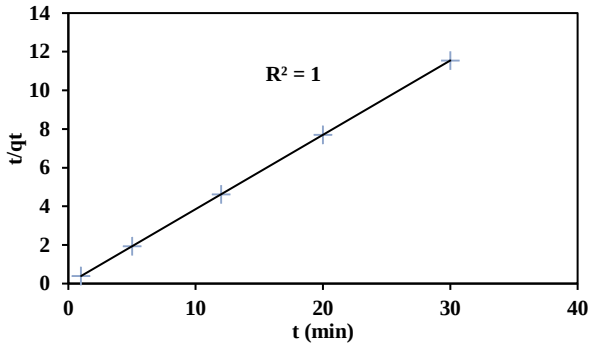

Fig. 11 Pseudo-second-order kinetic model of vanadium adsorption

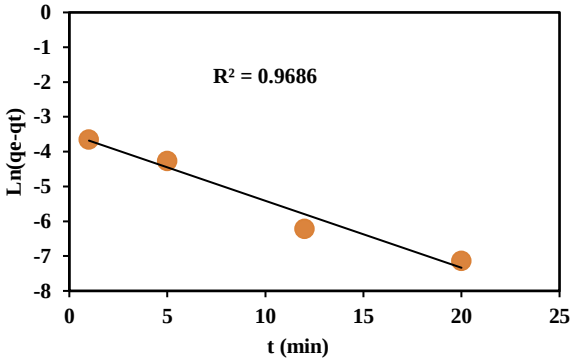

Fig. 12 Pseudo-first-order kinetic model of vanadium adsorption

contact time and the data obtained are shown in Fig. 10. Therefore, the time effect on the adsorption process was studied. The effect of contact time on the adsorption capacity of V(V) is shown in Table 2. It can be seen that the adsorption process is relatively fast and the equilibrium is reached after about 1 min.

The kinetics of magnetite adsorbent is very fast compared to other adsorbents such as zeolite and activated carbon adsorbent, which has provided an adsorption percentage of 98.6 in the minimum contact time. In the study of the previous parameter, the time of the shaker device was set to 30 minutes, and the adsorption rate was 98.6 to 100% repeatable, and in the study of the contact time parameter, we achieved the same adsorption percentage with a time of 30 minutes. Therefore, this time was used for the proper adsorption of vanadium in subsequent studies. Most adsorption reactions are controlled by a number of successive steps including: (a) resistance to film diffusion, (b) resistance to intraparticle diffusion, and (c) the proper sorption reaction rate [37,40]. Since the first step is excluded by sufficient shaking the solution, the rate determining step is one of the other two steps. To better understand the adsorption kinetics, various equations such as the Pseudo First Order (PFO), the Pseudo-Second Order (PSO) and The Resistance to Intraparticle Diffusion (RID) were used to model the kinetic data [41-43].

Weber and *Morris* (1962) expressed the intraparticle diffusion model as shown in Eq. (4):

$$q_t = K_{dif} t^{1/2} + C \quad (4)$$

Where: C is the intercept; K_{dif} $(mg/g\ \ h^{1/2})$, the intraparticle diffusion rate constant; q, the amount of solute adsorbed per unit weight of adsorbent per time (mg/g); $t^{1/2}$ the half-adsorption time $(h^{1/2})$. The intercept of the plot reflects the boundary layer effect. For intraparticle diffusion to be the only rate-determining step, then the regression of q_t against $t^{1/2}$ must be linear and should pass through the origin. If otherwise, then it implies that the intraparticle diffusion is not the only rate-controlling step [44].

were used to model the kinetic data. The linear forms of PFO and PSO models are expressed in Eq. 5 and Eq. 6, respectively:

$$ln(q_e - q_t) = lnq_e - k_1 t \quad (5)$$

$$\frac{t}{q_t} = \frac{1}{k_2 q_e^2} + \frac{t}{q_e} \quad (6)$$

Where q_e and q_t (mg/g) refer to the amount of V(V) adsorbed at equilibrium and at time (t), respectively; k_1 $(min^{-1}\ )$ and k_2 (g/$(mg\ \ .\ min\ \ )$ are the rate constant of PFO and PSO models, respectively. The values of model parameters $(k_1,\ k_2,\ q_e)$ can be calculated from the linear plots of $ln(q_e - q_t)$ versus t and $\frac{t}{q_t}$ versus.

The adsorption kinetics of vanadium ions by magnetite nanoparticle adsorbent was well fitted by the pseudo-first-order model and the pseudo-second-order model, but the fitting coefficient of the line with the pseudo-second-order

Table 3: Values of kinetic parameters of V(V) adsorption on bare magnetite nanoparticles

Kinetic models	Parameters		
Pseudo-first-order	$q_{e,cal}(mg/g)$ 2.5980	$k_1(min)^{-1}$ 0.1922	R^2 0.9686
Pseudo-second-order	$q_{e,cal}(mg/g)$ 2.60	$k_1(g/mg)(min)$ 40.00	R^2 1

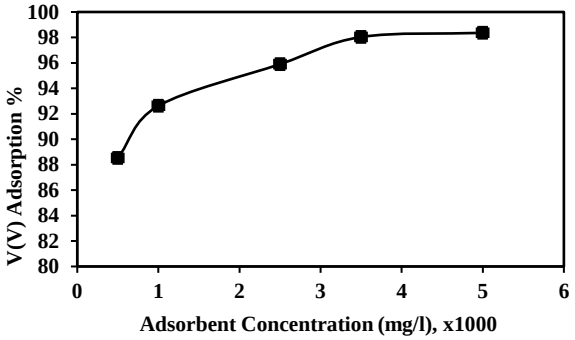

Fig. 13: Effect of adsorbent on vanadium separation ($C_0(V)$ = 50 mg/L; t= 30 min; T = room temperature; pH = 3.5)

model in Fig. 11 was equal to 1, while the fitting coefficient of the line with the pseudo-first-order model in Fig. 12, it was equal to 0.9686. Therefore, by matching the data with the pseudo-second-order model diagram, the adsorption kinetics of vanadium ions by the adsorbent was analyzed with the pseudo-second-order kinetic model. Based on these experiments, the kinetic parameters of the adsorption process for V(V) metal ion was calculated, and the results are reported in Table 3.

In order to evaluate the contribution of intraparticle diffusion on the control of uptake kinetic, the data was treated using a simplified RID Eq. (7) [43]:

$$q_t = k_{int} t^{1/2} + c \quad (7)$$

Where k_{int} is the intraparticle diffusion rate constant. The k_{int} can be calculated from the slope of the regression line of q_t versus $t^{1/2}$.

Effect of adsorbent dosage on vanadium separation

The optimum amount of magnetite nanoparticles for maximum adsorption and separation of vanadium at pH 3.5 was determined by changing the amount of adsorbent from 500 mg/L to 5000 mg/L. The results of this study are presented in Fig. 13. The results showed that the percentage of vanadium separation increased with the increase of adsorbent concentration up to 3500 mg/L (this means that the removal efficiency showed direct relationship with adsorbent amount), and after that the concentration of vanadium separation remained almost constant. The result is that as the amount of adsorbent increases, the surface area and adsorption sites of the magnetite nanoparticles available for the adsorption of vanadium ions increase, thereby increasing the adsorption of vanadium. So it leads to more efficient adsorption. An increase in dosage of adsorbent can provide the additional active sites and/or greater surface area for the efficient adsorption of the metal ions at a fixed initial concentration. According to Fig. 13, the maximum adsorption of V(V) ion took place at dose of 3500 mg/L, and significant changes were not observed at higher increase in adsorbent dosage. Beyond 5000 mg/L, the formation of aggregates and consequent self-binding of adsorbent particles might decrease the active sites of adsorbent at higher doses. These findings are in good agreement with previous studies for several sorbent-metal sorption studies (*Zeinali et al.* [23]; *Kordparijaei et al.* [26]). To ensure the maximum amount of adsorption, the amount of 5000 mg/L of adsorbent with 99.6% adsorption and separation of this metal was selected as the optimal amount of adsorbent for conducting the subsequent experiments.

Effect of adsorption temperature

The temperature effect on V(V) adsorption was tested as function of 4 temperature degrees (20, 30, 40 and 50 °C). As shown in Fig. 14, the increase in temperature that leads to an increase in the percentage of vanadium adsorbed on the adsorbent surface may be attributed to changes in the adsorbent surface properties. Since the removal efficiency reached 98.42 percent at room temperature (20 °C), increasing the temperature did not result in a significant numerical difference in the adsorption of vanadium in the adsorption process, and since all experiments were performed at room temperature. Therefore, to determine the optimal value of this parameter for subsequent experiments and repeatability of experiments, the temperature of 20 °C (room temperature) was selected.

Table 4: Thermodynamic parameters for vanadium adsorption on magnetite nanoparticles

ΔG°(KJ/mol)			ΔH°(KJ/mol)	ΔS° (J/mol)
293.15 (K)	303.15 (K)	313.15 (K)	+20.24	+96
-28.1	-29	-30		

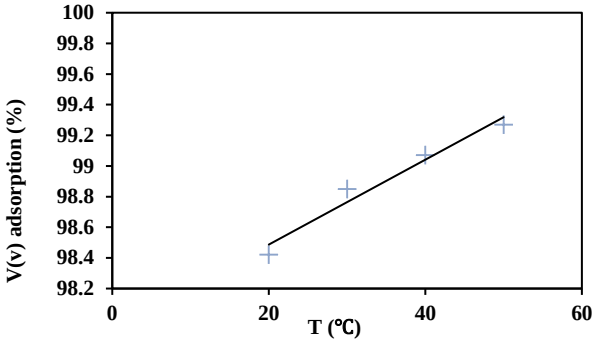

Fig. 14: Effect of temperature on vanadium separation ($C_0(V)$ = 50 mg/L; t:30 min; pH = 3.5; sorbent dosage= 0.05 g.L^{-1})

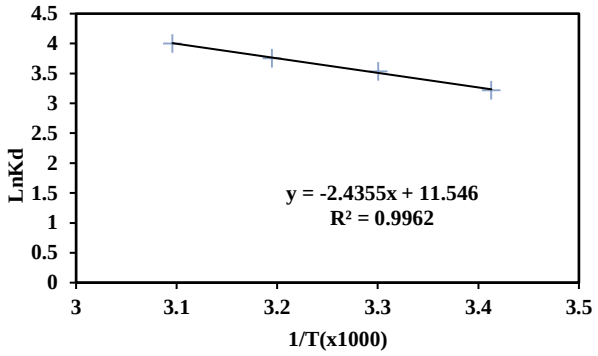

Fig. 15: Changes in the distribution coefficient in terms of temperature for the adsorption of vanadium ions on magnetite nanoparticles

ADSORPTION THERMODYNAMICS

The thermodynamics such as enthalpy (ΔH°, KJ/mol), entropy (ΔS°, J (mol/K)), and Gibbs free energy (ΔG°, KJ/mol) of vanadium sorption were determined by correlation of the equilibrium constant according the Van't Hoff equations which are placed in Eq. (8) and Eq. (9). [45]:

$$Ln\ K_L = -\frac{\Delta H^\circ}{RT} + \frac{\Delta S^\circ}{R} \quad (8)$$

$$\Delta G^\circ = \Delta H^\circ - T\Delta S^\circ \quad (9)$$

Where *R* is the gas constant, *T* the solution temperature (K) and K_L is the Langmuir equilibrium constant (L/mol). ΔH° and ΔS° were obtained from the slope and intercept of the linear Van't Hoff plots of ln K_L versus 1/T respectively. The diagram of $Ln\ K_L$ in terms of T/1 is shown in Fig. 15. Fig. 15 shows a line with very good correlation coefficients (R^2=0.9971). Table 4. shows the results of thermodynamic and kinetic parameters. The negative value of ΔG indicates that the adsorption reaction is thermodynamically possible and confirms that the adsorption process is physicochemical. (Adsorption of 0 and -20 kJ/mol indicates physical adsorption, -20 to -80 kJ/mol indicates physicochemical adsorption, and -80 to -400 kJ/mol indicates chemical adsorption). According to the values of free energy change (ΔG) which was negative and decreased with increasing temperature, this article shows that the adsorption of vanadium to the magnetite adsorbent is spontaneous and the adsorption at a higher temperature is more favorable.

The positive enthalpy indicates that the adsorption process of vanadium with magnetite nanoparticles is an endothermic process. Meanwhile, it also confirms that the adsorption process is physicochemical. Finally, the positive entropy value confirms that the adsorption reaction at the liquid/solid phase interface for vanadium adsorption using magnetite adsorbent is completely random and also indicates that the degree of randomness at the solid-liquid interface increased during adsorption. This randomness is due to the destruction of the hydration shell of vanadium ions, which provides surface adsorption of the adsorbent. Therefore, it is concluded that the adsorption process of vanadium on magnetite nanoparticles is a spontaneous, endothermic and physicochemical process which was consistent with some studies (*Gdula et. al* [24]; *Abd El-Magied et. al* [46]).

.

Study of Vanadium adsorption isotherms

Adsorption equilibrium information is the most important piece of information needed to properly understand the adsorption process. Proper understanding and interpretation of adsorption isotherms is essential for overall improvement of adsorption mechanism pathways and effective adsorption system design. To check the equilibrium adsorption isotherm, the diagram of adsorbed vanadium ions (q_e) according to the equilibrium concentration of vanadium ions in the solution (C_e) is

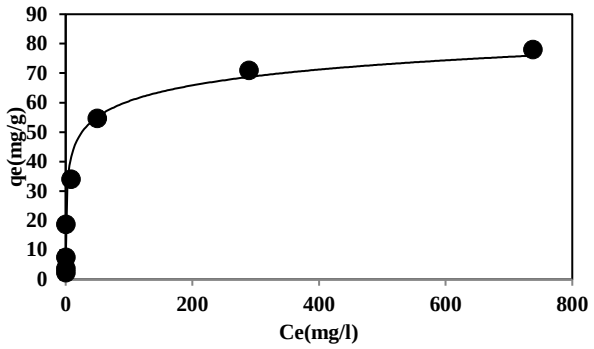

Fig. 16: Adsorption isotherm of vanadium (Volume = 0.02 L; $C_0(V)$ = 6-933 mg/L; pH= 3.5; T = room temperature; t = 30 min.; sorbent dosage= 0.05 g/L)

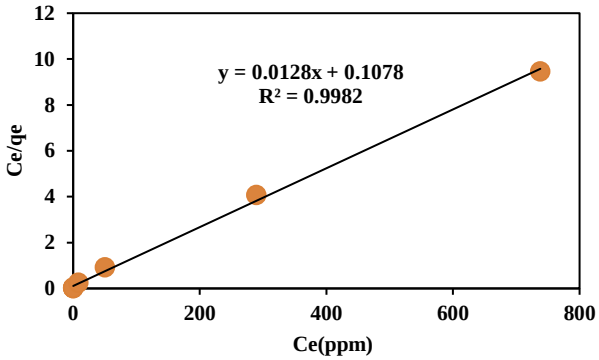

Fig. 17: Langmuir adsorption isotherm

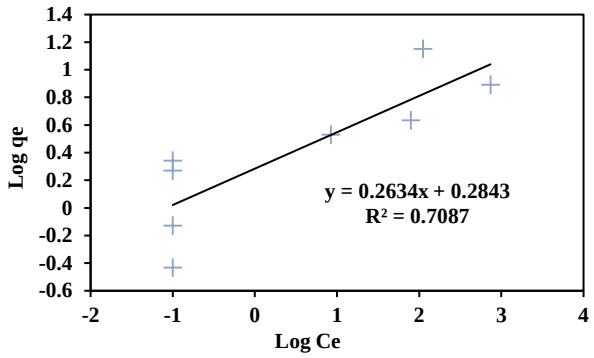

Fig. 18: Freundlich adsorption isotherms

drawn and presented in Fig. 16, while the equations of Langmuir, Freundlich and Temkin isotherms for adsorption Vanadium was studied by bare magnetite nanoparticles.

The adsorption isotherm represents the distribution of the solute between liquid and solid phases at equilibrium at constant temperature. A relation between the amount of adsorbate adsorbed on a given surface at constant temperature and the equilibrium concentration of the substrate in contact with the adsorbent is known as adsorption isotherm. Adsorption isotherms depend on certain parameters, which its values express the surface properties and the affinity of the sorbent. [47,48]. We can compute experimental results from equilibrium experiences by several adsorption isotherm models.

(1) Langmuir Model: The most widely used isotherm equation for modeling equilibrium data is the Langmuir model. Langmuir derived a relation between adsorbed material and its equilibrium concentration [49,50]. The linear form of Langmuir equation is given by Eq. 10.

$$\frac{C_e}{q_e} = \frac{1}{Q_{max}K_L} + \frac{1}{q_{max}}C_e \qquad (10)$$

where C_e is the equilibrium concentration of ions in solution (mg/L), q_e is the amount adsorbed at Ce (mg/g), Q_{max} is the maximum adsorption capacity (mg/g), and K_L is the binding constant which is related to the energy of adsorption (L/mg). According to Fig. 17 Plotting C_e/q_e against C_e gives a straight line with slope and intercept equal to $\frac{1}{Q_{max}}$ and $\frac{1}{K_L}$, respectively. The values of K_L and Q_{max} increase as the temperature increases. Increasing of K_L value with increasing of temperature implies the strong binding between V(V) ions and the active sites at elevated temperatures.

(2) Freundlich Model: The Freundlich isotherm model [50,51] is an empirical relationship that describes the sorption of solutes on a solid surface assuming that different sites with several sorption energies are involved (the surface of adsorbent is heterogeneous). This isotherm model is given by Eq. (11).

$$\log q_e = \log K_F + \frac{1}{n}\log C_e \qquad (11)$$

Where q_e (mg/g) and C_e (mg/L) are the equilibrium concentrations of V(V) in the solid and liquid phase, respectively. K_F (mg/g) and n are characteristic constants related to the relative sorption capacity of the sorbent and the intensity of sorption, respectively. The higher the $\frac{1}{n}$ value is, the more favorable the adsorption is; generally, n<1. $\frac{1}{n}$ and $\log K_F$ are the slope and intercept, respectively, given by plotting$\log q_e$ against $\log C_e$. According to Fig. 18 the Freundlich plot gave a slope less than unity indicating the nonlinear sorption behavior with V(V) in the concentration range studied.

The values of equilibrium sorption capacity and correlation coefficients of Langmuir equation (Q_{max}) are

Table 5: isotherm model parameters for adsorption of V(V) by magnetite nanoparticles

Temkin's Model			Freundlich Model			Langmuir Model		
R^2	$K_T\ (\frac{L}{mg})$	b	R^2	$K_F(\frac{mg}{g})(\frac{mg}{L})^{1/n}$	n	R^2	$K_L\ (\frac{L}{mg})$	$q_L\ (\frac{mg}{g})$
0.6332	$1.44 \times 10^{+13}$	243	0.7087	13.3	3.0	0.9982	0.12	78

Table 6: The maximum adsorption capacity of monolayer V(V) and U(VI) of some reported adsorbents

Adsorbent	Ion	q_m (mg/g)	References
HA/Fe_3O_4	V(V)	8.97	[23]
$AC\_Fe_3O_4$	U(VI)	15.87	[52]
Magnetic baggas	U(VI)	32.4	[53]
$CeO_2 - TiO_2 - Fe_2O_3$	U(VI)	40	[54]
Magnetic chitosan	U(VI)	42	[55]
Magnetic chitosan modified with humic acid	U(VI)	47.9	[56]
Magnetic Zeolite-Polymer Composite	V(V)	57.803	[57]
Polypyrrole coated magnetize d natural zeolite	V(V)	74.9	[33]
Bare Magnetite Nanoparticles	V(V)	78	Present work

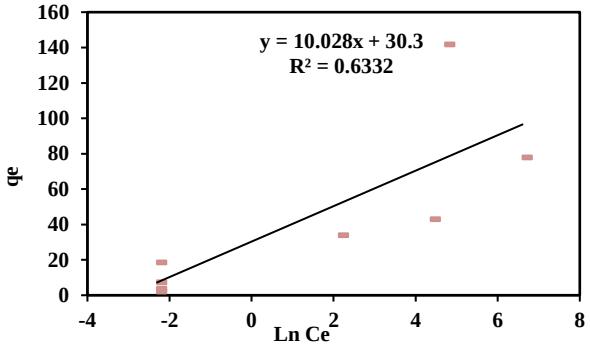

Fig. 19: Temkin adsorption isotherms

more consistent with the experimental data than Freundlich isotherm model (Similar to the studies of *Zeinali et al.* [23]; *Kordparijaei et al.* [26]). Therefore, the sorption reaction is more favorable by Langmuir model.

(3) Temkin's Model: The derivation of the Temkin isotherm assumes that the fall in the heat of sorption is linear rather than logarithmic, as implied in the Freundlich equation [48,49]. The linear form of Temkin isotherm is given by the Eq. 12.

$$q_e = \frac{RT}{b} lnA_T + \frac{RT}{b} lnC_e \quad (12)$$

where A_T is Temkin isotherm equilibrium binding constant (L/g), b is Temkin isotherm constant, R is universal gas constant (8.314 J/mol.K), T is temperature at 298 K, and B is constant related to heat of sorption (J/mol), where q_e (mg $.g^{-1}$) and C_e (mg $.L^{-1}$) are the equilibrium concentrations of V(V) in the solid and liquid phase, respectively. According to Fig. 19 plotting q_e versus ln C_e should give a straight line if the adsorption energy decreases linearly with increasing surface coverage. The parameters for these models and the coefficient values are shown in Table 5.

Comparison of the adsorption capacity of various adsorbents

The maximum adsorption capacity (q_m) of bare magnetite nanoparticles was compared with the adsorption results reported in some papers using several adsorbents., as depicted in Table 6. The obtained q_m values for V(V) ion was greater than those reported for other adsorbents. The obvious advantage of the current research project was that without functionalizing the adsorbent, we were able to achieve a very good and higher adsorption capacity than the functionalized adsorbents listed in Table 6. In addition, it should be noted that eliminating the adsorbent functionalization step leads to saving time and simplifying the synthesis process which is suitable for industrial works that seek simple and uncomplicated synthesis processes. One of the reasons for the functionalization of adsorbents is to increase the selectivity of the adsorbent, but in the present project, without functionalizing the adsorbent, we were able to achieve almost good results in the selectivity test for vanadium and uranium.

Table 7: desorption of vanadium by magnetite nanoparticle with using of different concentration of $(NH_4)_2CO_3$ and NH_4HCO_3

stripping agents (M)		Percentage of vanadium desorption
ammonium carbonate	0.5	93.3
ammonium bicarbonate	0.2	95.4
	0.5	91.2
	0.7	92.0
	1	91.6

Table 8: Selectivity of adsorbent

	V				U				Fe			
pH	$C_i(\frac{mg}{l})$	$C_f(\frac{mg}{l})$	Extraction (Percent)	K_d	$C_i(\frac{mg}{l})$	$C_f(\frac{mg}{l})$	Extraction (Percent)	K_d	$C_i(\frac{mg}{l})$	$C_f(\frac{mg}{l})$	Extraction (Percent)	K_d
1.5	8.2	0.63	92.3	343.3	8.8	4.4	50	28.6	7.6	48	-531.6	-24
3.5	14	0.95	93.2	392.5	11.7	4.3	63.2	49.2	5.8	95.4	-1544.8	-26.8
7	8.2	1.37	83.3	4.142	8.8	3.3	62.5	47.6	7.6	12	-57.9	-10.5

Investigation of desorption of Vanadium from adsorbent

It was observed that the adsorbent with magnetite core under the mentioned optimal conditions was able to adsorb more than 99.6% of vanadium from the aqueous solution. Therefore, the study of separation with this adsorbent entered subsequent study. To do this, vanadium was adsorbed from the solution under optimal separation conditions obtained from the previous steps, and then the vanadium containing adsorbent entered the desorption step. At this stage, the separation of vanadium from the adsorbent was studied using stripping agents including sulfuric acid, ammonium bicarbonate and ammonium carbonate. sulfuric acid could strip a relatively lower percentage of vanadium than the other two stripping agents. Thus, different concentrations of the other two stripping agents, namely ammonium bicarbonate and ammonium carbonate, were investigated. The results of this study are presented in the Table 7.

Selective separation effect

To investigate the effect of the presence of different ions in the solution containing vanadium on the separation of vanadium, the study was performed under optimal extraction conditions at pH 1.5, 3.5 and 7.0. Standard ICP solutions (uranium and iron) with vanadium were used for this purpose. The final volume of the experiments was adjusted to 20 mL (10 mL of the volume of solution to be extracted plus 10 mL of magnetite nanoparticle adsorbent at a concentration of 7000 mg/L) in a test tube and the pH of the solution to the desired values. Table 8. shows the amount of metal extraction at pH 1.5, 3.5 and 7.0. From these results, it is obvious that increasing other metal ions at neutral pH (pH 7.0) has reduced the vanadium separation, which is not significantly different from the values extracted under optimal extraction conditions without the presence of other ions. Separation of vanadium at more acidic pH (pH equal to 1.5 and 3.5) also changed to less than normal extraction under optimal conditions. It is noteworthy that despite the high adsorption of vanadium, the adsorption of another element, uranium was relatively good and more than 50%, which indicates the high adsorption capacity of the adsorbent for this group of heavy metals. According to Table 8. the unusual results obtained from iron metal ions with this adsorbent in the mentioned conditions were due to the adsorbent material. Iron adsorption was adsorbed by the adsorbent. The appropriate solution to this problem is to increase the concentration of iron ions in the solution relative to the concentration of iron in the adsorbent so that if some iron in the adsorbent enters the solution, there will be no problem in adsorbing the ions in solution. Due to the complexity of the extraction conditions of the elements as well as the preparation of the adsorbent for the separation of elements and other metals, it is necessary to conduct more detailed studies on this issue.

CONCLUSIONS

Vanadium separation studies were performed by adsorption of non-functionalized magnetite nanoparticles under optimal conditions, pH 3.5 and with a rapid kinetics

at an optimal time of 30 minutes, more than 99.6 percent vanadium was removed from the solution. The adsorption model showed good agreement with the Langmuir adsorption isotherm and showed the separation capacity of vanadium with these particles was 78 mg/g. The kinetics of the experiment displayed that the data obtained were more consistent with the pseudo-second-order kinetic model. The results of thermodynamic calculation indicated that the reaction is endothermic ($\Delta H° > 0$), spontaneous ($\Delta G° < 0$) and increased randomness ($\Delta S° > 0$) during adsorption. The pH parameter and the initial vanadium concentration were considered as an important parameters. Vanadium desorption studies from the surface of the particles showed that the highest amount, i.e. 95.42 percent, is obtained by ammonium bicarbonate with a concentration of 0.2 M. Separation of vanadium in the presence of iron and uranium cations at pH 1.5, 3.5 and 7.0 showed that 92.3, 93.2 and 83.3 percent of vanadium were extracted, respectively. It seems that by changing the pH conditions, vanadium can be separated from other associated elements. This issue requires further investigation.

Acknowledgments

We acknowledge the Nuclear Fuel Cycle Research Institute, Nuclear Science and Technology Research Institute as providers of financial sum, facilities, contributors, etc.

Received : Dec. 02, 2022 ; Accepted : Mar. 06, 2023

REFERENCES

[1] Li M., Zhang B.G., Zou S.Q., Liu Q.S., Yang M., Highly Selective Adsorption of Vanadium (V) by Nano-Hydrous Zirconium Oxide-Modified Anion Exchange Resin, *Journal of Hazardous Materials*, **384**:121386 (2020).

[2] Wen J., Jiang T., Zheng X., Wang J., Cao J., Zhou M., Efficient Separation of Chromium and Vanadium by Calcification Roasting–Sodium Carbonate Leaching from High Chromium Vanadium Slag and V_2O_5 Preparation, *Sep. Purif. Technol.*, **230**:115881 (2020).

[3] Peng H., A Literature Review on Leaching and Recovery of Vanadium, *J. Environ. Chem. Eng.*, **7**:103313 (2019).

[4] Li H., Wang C., Lin M., Guo Y., Xie B., Green One-Step Roasting Method for Efficient Extraction of Vanadium and Chromium from Vanadium-Chromium Slag, *Powder Technol.*, **360**:503-508 (2020).

[5] Gilligan R., Nikoloski A.N., The Extraction of Vanadium from Titanomagnetites and Other Sources, *Miner. Eng.*, **146**: 106106 (2020).

[6] Tian L., Xu Z., Chen L., Liu Y., Zhang T.A., Effect of Microwave Heating on the Pressure Leaching of Vanadium from Converter Slag, *Hydrometallurgy*, **184**: 45–54 (2019).

[7] Yang Q.w., Xie Z.m., Peng H., Liu Z.h., Tao C.Y., Leaching of Vanadium and Chromium from Converter Vanadium Slag Intensified with Surface Wettability, *J. Cent. South. Univ.*, **25(6)**: 1317–1325 (2018).

[8] Traceyc S.A., Willsky G.R., Takeuchi E.S., "Chemistry, Biochemistry, Pharmacology and Practical Applications", 1st Edition. CRC Press, Boca Raton, (2007).

[9] Guzman j., Saucedo L., Navarro R., Revilla j., Guibal E., Vanadium Interactions with Chitosan: Influence of Polymer Protonation and Metal Speciation, *Langmuir*, **18**:1567-1573 (2002).

[10] Giovanni C., Chiara D., Angela A., Grasso R., Fallico S., Sciacca M., Fiore M., Ferrante J., Determination of Total Vanadium and Vanadium(V) in Groundwater from Mt. Etna and Estimate of Daily Intake of Vanadium(V) through Drinking Water, *Water Health*, **13**: 522–530 (2015).

[11] X Zhu., Liu Y., Li W., Efficient Separation and Recovery of Vanadium(V) from Hydrochloric Acid Solution Using N1923 as an Extractant, *ACS Omega*, **7(6):**5485–5494 (2022).

[12] Rizk S.E., Hamed M.M., Batch sorption of Iron Complex Dye, Naphthol Green B, from Wastewater on Charcoal, Kaolinite, and Tafla, *Desalin. Water. Treat*, **56**: 1536–1546 (2015).

[13] He Q., Si S., Zhao J., Yan H., Sun B., Cai Q., Yu Y., Removal of Vanadium from Vanadium-Containing Wastewater by Amino Modified Municipal Sludge Derived Ceramic, *Saudi. J. Biol. Sci.*, **25**: 1664–1669 (2018).

[14] Babel S., Kurniawan T.A., Low-Cost Adsorbents for Heavy Metals Uptake from Contaminated Water: A Review, *J. Hazard. Mater*, **97**: 219–243(2003).

[15] Al Abdullah J., Al Lafi A., Alnama T., Al Masri W., Amin Y., Alkfri M., Adsorption Mechanism of Lead on Wood/Nano-Manganese Oxide Composite, *Iran. J. Chem. Chem. Eng. (IJCCE)*, **37(4)**: 131-144 (2018).

[16] Saleem J., Shahid U.B., Hijab M., Mackey H., McKay G., Production and Applications of Activated Carbons as Adsorbents from Olive Stones, *Biomass Convers. Biorefin*, **9**: 775–802 (2019).

[17] Mardvar A., Hajiaghababaei L., Allahgholi Ghasri M., Dehghan Abkenar S., Badiei A., Ganjali M., Mohammadi Ziarani G., Simultaneous Removal of Pb^{2+} and Cu^{2+} by SBA-15/di-Urea as a Nano Adsorbent, *Iran. J. Chem. Chem. Eng. (IJCCE)*, **41(1)**: 163-173 (2022).

[18] Kumar R., Rauwel P., Rauwel E., Nanoadsorbants for the Removal of Heavy Metals from Contaminated Water: Current Scenario and Future Directions, *Processes*, **9(8)**:1379 (2021).

[19] Carmen I., Filip P., Humelnicu D., Humelnicu I., Scott T., Crane R., Removal of Uranium (VI) from Aqueous Systems by Nanoscale Zero-Valent Iron Particles Suspended in Carboxy-Methyl Cellulose, *Journal of Nuclear Materials*, **443(1-3)**: 250-255 (2013).

[20] Masteri Farahani M., Taghizadeh F., Molybdenum-Schiff Base Complex Immobilized on Magnetite Nanoparticles as a Reusable Epoxidation Catalyst, *Iran. J. Chem. Chem. Eng. (IJCCE)*, **37(6)**: 35-42 (2018).

[21] Tamjidi S., Esmaeili H., Kamyab Moghadas B., Application of Magnetic Adsorbents for Removal of Heavy Metals from Wastewater: A Review Study, *Mater. Res. Express*, **6(10)**: 102004 (2019).

[22] Etale A., Tutu H., Drake D.C., The Effect of Silica and Maghemite Nanoparticles on Remediation of Cu(II)-, Mn(II)- and U(VI)-Contaminated Water by Acutodesmus sp, *J. Appl. Phycol.*, **28**: 251–260 (2016).

[23] Zeinali S., Tatian S., Vanadium Removal from Fuel Oil and Waste Water in Power Plant Using Humic Acid Coated Magnetic Nanoparticles, *Int. J. Nanosci. Nanotechnol*, **15**(4): 249-263 (2019).

[24] Gdula K., Gładysz Płaska A., Cristóvão B., Ferenc W., Skwarek E., Amine-Functionalized Magnetite-Silica Nanoparticles as Effective Adsorbent for Removal of Uranium(VI) ions, *Journal of Molecular Liquids*, **290**: 111217 (2019).

[25] Omidinasab M., Rahbar N., Ahmadi M., Kakavandi B., Ghanbari F., Kyzas G.Z., Martinez S.S., Jaafarzadeh N., Removal of Vanadium and Palladium Ions by Adsorption onto Magnetic Chitosan Nanoparticles, *Environmental Science and Pollution Research*, **25**: 34262- 34276 (2018).

[26] Kord Parijaee M., Noaparast M., Saberyan K., Shafaie Tonkaboni S.Z., Adsorption of Vanadium(V) from Acidic Solutions by Using Octylamine Functionalized Magnetite Nanoparticles as a Novel Adsorbent, *Korean Journal of Chemical Engineering*, **31**: 2237-2244 (2014).

[27] Zhang J., Lin S., Han M., Su Q., Xia L., Hui Z., Adsorption Properties of Magnetic Magnetite, *Water*, **12(2)**: 446 (2020).

[28] Ahmed M.A., Ali S.M., El-Dek S.I., Galal A., Magnetite–Hematite Nanoparticles Prepared by Green Methods for Heavy Metal Ions Removal from Water, *Materials Science and Engineering: B*, **178(10)**: 744-751 (2013).

[29] Chowdhury S.R., Yanful E.K., Pratt A.R., Chemical states in XPS and Raman Analysis During Removal of Cr(VI) from Contaminated Water by Mixed Maghemite–Magnetite Nanoparticles, *Journal of Hazardous Materials*, **235-236** :242-256 (2012).

[30] Xu J, Zhou L, Jia Y, Liu Z, Adesina A.A., Adsorption of Thorium (IV) Ions from Aqueous Solution by Magnetic Chitosan Resins Modified with Triethylene-Tetramine, *Journal of Radioanalytical and Nuclear Chemistry*, **303**: 347–356 (2015).

[31] Amani V., Ahmadi R., Naseh M., Ebadi A., Synthesis, Spectroscopic Characterization, Crystal Structure and thermal Analyses of two Zinc(II) Complexes with Methanolysis of 2-Pyridinecarbonitrile as a Chelating Ligand, *Journal of the Iranian Chemical Society*, **14**: 635-642 (2017).

[32] Bhattacharya K., Deb P., Hybrid Nanostructured C-Dot Decorated Fe3O4 Electrode Materials for Superior Electrochemical Energy Storage Performance, *Dalton Trans*, **44**: 9221–9229 (2015).

[33] Mthombeni N.H., Mbakop S., Ochieng A., Onyango M.S., Vanadium (V) Adsorption Isotherms and Kinetics Using Polypyrrole Coated Magnetized Natural Zeolite, *Journal of the Taiwan Institute of Chemical Engineers*, **66**: 172-180 (2016).

[34] Ahamadi M., Hazrati Niari M., Kakavandi B., Development of Maghemite Nanoparticles Supported on Cross-Linked Chitosan (γ-Fe2O3@CS) as a Recoverable Mesoporous Magnetic Composite for Effective Heavy Metals Removal, *Journal of Molecular Liquids*, **248**: 184-196 (2017).

[35] Liu X., Zhang L., Insight Into the Adsorption Mechanisms of Vanadium(V) on a High-Efficiency Biosorbent (Ti-Doped Chitosan Bead), *International Journal of Biological Macromolecules*, **79**: 110- 117 (2015).

[36] Peacock K., Sherman D., Vanadium(V) Adsorption onto Goethite (α-FeOOH) at pH 1.5 to 12: a Surface Complexation Model Based on ab Initio Molecular Geometries and EXAFS Spectroscopy, *Geochimica et Cosmochimica Acta*, **68(8)**: 1723-1733 (2004).

[37] Hao P., Hongzhi Q., Caiqiong W., Binfang Y., Huisheng H., Bing L., Thermodynamic and Kinetic Studies on Adsorption of Vanadium with Glutamic Acid, *ACS Omega*, **6**: 21563−21570 (2021).

[38] Nayl A.A., Aly H.F., Solvent Extraction of V(V) and Cr(III) from Acidic Leach Liquors of Ilmenite Using Aliquat 336, *Transactions of Nonferrous Metals Society of China*, **25(12)**: 4183-4191 (2015).

[39] Zhang J., Lin S., Han M., Su Q., Xia L., Hui Z., Adsorption Properties of Magnetic Magnetite Nanoparticle for Coexistent Cr(VI) and Cu(II) in Mixed Solution, *Water*, **12(2)**: 446 (2020).

[40] Mohadesi M., Moradi G., Davvodbeygi Y., Hosseini S., Soybean Oil Transesterification Reactions in the Presence of Mussel Shell: Pseudo-First Order Kinetics, *Iran. J. Chem. Chem. Eng. (IJCCE)*, **37(4)**: 43-51 (2018).

[41] Monier M., Ayad D.M., Wei Y., Sarhan A.A., Adsorption of Cu(II), Co(II), and Ni(II) Ions by Modified Magnetic Chitosan Chelating Resin, *Journal of Hazardous Materials*, **177**: 962–970 (2010).

[42] Xu J., Zhou L., Jia Y., Liu Z., Adesina A.A., Adsorption of Thorium (IV) Ions from Aqueous Solution by Magnetic Chitosan Resins Modified with Triethylene-Tetramine, *Journal of Radioanalytical and Nuclear Chemistry*, **303**: 347–356 (2015).

[43] Atia A.A., Donia A.M., Elwakeel K.Z., Recovery of Gold(III) and Silver(I) on a Chemically Modified Chitosan with Magnetic Properties, *Hydrometallurgy*, **87**: 197–206 (2007).

[44] Wu R., Qu J., Chen Y., Magnetic Powder MnO–Fe_2O_3 Composite—A Novel Material for the Removal of Azo-Dye from Water, *Water Research*, **39(4)**: 630-638 (2005).

[45] Zhang X., Jiao C., Wang J., Liu Q., Li R., Yang P., Zhang M., Removal of uranium(VI) from aqueous Solutions by Magnetic Schiff Base: Kinetic and Thermodynamic Investigation, *Chemical Engineering Journal*, **198**:412–419 (2012).

[46] Abd El Magied M.O., Sorption of Uranium Ions from Their Aqueous Solution by Resins Containing Nanomagnetite Particles, *Journal of Engineering*, **2016**(1):1-11 (2016).

[47] Donia A.M., Atia A.A., Moussa E.M.M., El-Sherif A.M., Abd El-Magied M.O., Removal of Uranium(VI) from Aqueous Solutions Using Glycidyl Methacrylate Chelating Resins, *Hydrometallurgy*, **95**(3-4):183–189 (2009).

[48] Dong W., Brooks S.C., Determination of the Formation Constants of Ternary Complexes of Uranyl and Carbonate with Alkaline Earth Metals (Mg^{2+}, Ca^{2+}, Sr^{2+}, and Ba^{2+}) Using Anion Exchange Method, *Environmental Science & Technology*, **40(15):** 4689–4695 (2006).

[49] Xiong C., Liu X., Yao C., Effect of pH on Sorption for RE(III) and Sorption Behaviors of Sm(III) by D152 Resin, *Journal of Rare Earths*, **26(6):** 851–856 (2008).

[50] Dada A.O., Olalekan A.P., Olatunya A.M., Dada O., Langmuir, Freundlich, Temkin and Dubinin–Radushkevich Isotherms Studies of Equilibrium Sorption of Zn 2+ Unto Phosphoric Acid Modified Rice Husk, *Journal of Applied Chemistry*, **3**(1):38–45 (2012).

[51] Mpofu V.P., Addai Mensah J., Ralston J., Temperature Influence of Nonionic Polyethylene Oxide and Anionic Polyacrylamide on Flocculation and Dewatering Behavior of Kaolinite Dispersions, *Journal of Colloid and Interface Science*, **271(1)**: 145–156 (2004).

[52] Akbari Jonoush Z., Farzadkia M., Naseri S., Mohajerani H., Esrafili dizaji A., Dadban Shahamat Y., Removal of Uranium (VI) from aqueous solution by Uranium Benzamide Complex using AC_Fe_3O_4 Nanocomposite, *International Journal of Hydrogen Energy*, **7(4)**: 499-510 (2015).

[53] Milani S.A., Rahnama B., Darban A.K., Adsorptive Removal and Recovery of U(VI) from Single Component Aqueous Solutions by Sugarcane Bagasse Impregnated with Magnetite Nanoparticles, *J. of Nuclear Sci. and Tech.*, **35(67)**: 49-62 (2014).

[54] El Sherif R M., Lasheen T.A., Jebril E.A., Fabrication and Characterization of CeO_2-TiO_2-Fe_2O_3 Magnetic Nanoparticles for Rapid Removal of Uranium ions from Industrial Waste Solutions, *Journal of Molecular Liquids*, **241**: 260-269 (2017) .

[55] Cláudio L., Stopa L., Yamaura M., Uranium Removal by Chitosan Impregnated with Magnetite Nanoparticles: Adsorption and Desorption, *International Journal of Nuclear Energy Science and Technology*, **5(4)**: 283-289 (2010).

[56] Basu H., Saha S., Pimple M.V., Singhal R.K., Novel Hybrid Material Humic Acid Impregnated Magnetic Chitosan Nano Particles for Decontamination of Uranium from Aquatic Environment, *Journal of Environmental Chemical Engineering*. **7(3)**: 103110 (2019).

[57] Mthombeni N.H., Mbakop S., Onyango M.S., Magnetic Zeolite-Polymer Composite as an Adsorbent for the Remediation of Wastewaters Containing Vanadium, *International Journal of Environmental Science and Development*, **6(8)**: 602-605 (2015).